Laboratório Nacional de Energia e Geologia, I.P.

UNIDADE DE ENERGIAS RENOVÁVEIS E INTEGRAÇÃO DE SISTEMAS DE ENERGIA

Porosity Effect in a Molten Salt Thermocline

Relatório interno

M. Giestas, P. Costa

2018

Porosity Effect in a Molten Salt Thermocline

M. Giestas, P. Costa

margarida.giestas@lneg.pt; paula.alexandracosta@lneg.pt;

LNEG - Est. do Paço do Lumiar 22, 1649-038, Lisboa, Portugal

Abstract

Thermal Energy Storage (TES) is essential for solar energy applications when the demand is not in phase with the supply of Solar Energy Molten salt thermocline storage tanks and can be a low cost option for thermal energy storage in Concentrating Solar Power (CSP) systems

To analyze the dynamics of a one tank a 2D already validated with data obtained from literature (Rojas, 2013) accounts separately for filler and molten salt regions due to their different thermos-physical properties. In the tank, between hot and cold zones a temperature gradient is established. This interface zone, called thermocline, is responsible for the whole performance of the storage tank.

Properties of fillers and molten salt can increase substantially the one tank efficiency by improving its stratification. This work analyses the particles size of filler in a specific set in order to account for the influence of this parameter in the performance of the storage thermocline tank. The work makes a review on the effect of the aspect ratio in the thermocline performance and ends with a mixture of the two influences

Keywords: Energy storage, Porosity, Voids, Aspect Ratio, Stratification.

Table of Contents

Table Index

Figures Index

Table 1 - Nomenclature

		Greek letters	
Cp [J/Kg ^{o}C]	Specific heat	α (m^2/s)	Thermal diffusivity
d [m]	Diameter of Thermocline tank	μ_t [Pa s]	Eddy viscosity
d_s [m]	Diameter of filler particles	ν (m^2/s)	Viscosity
d_m [m]	Mesh element size	ρ [kg/m^3]	Fluid specific mass
F	Inertial coefficient	ε	Porosity
K [m^2]	Permeability	Pe	Péclet number
$\vec{g}$ (m/s^2)	Gravity acceleration		
h [m]	Tank height	**Subscripts**	
h_i [W/m^3 ^{o}C]	Interstitial heat transfer coefficient.	0	Initial state
		s	solid
k [W/m ^{o}C]	Thermal conductivity	l	liquid
m [kg]	Mass	**Operators**	
p [Pa]	Pressure	∇	Gradient
T [^{o}C]	Temperature	$\nabla.$	Divergence
t [s]	Time	Δ	Laplacian operator
v [m/s]	Velocity field	**T**	Viscous Stress Tensor

1.Introduction

Thermal Energy Storage (TES) is essentially for solar energy applications, when the demand is not in phase with the supply of Solar Energy. These devices use typically two storage tank system, one for the Cold Liquid and another for the Hot Liquid.

The utilization of this two tanks structure, turns to be expensive and solutions using only one tank with a mixture of molten salt and a filler bed with a less expensive porous medium are a good alternative according to Angelini (Angelini G. *et al*, 2014) Two tanks devices are more efficient than one tank, but the potential reduction cost reduction of thermocline TES system is about 33%.

To obtain these two layers' stratification (hot fluid on top and cold fluid in the bottom) a thermocline region between the two layers must be maintained thin and with an intense temperature gradient. The thickness of this TES stratified tanks can operate effectively by exploiting the density difference of a single fluid at different temperatures. In this way the overall storage system tank turns to be economically attractive. A first concept of thermocline degradation considering a saturated porous media with a fluid was made by Gross (Gross, 1982).and Doug (Doug, 1986).

The properties of materials, are even more interesting in order to diminish the cost and improve the efficiency of a single tank. Tests made to different fillers by Kolb (Kolb et al., 2001) allowed to a better understanding of the parameters that affected the performance of a thermal storage system.

Thermocline degradation in saturated porous media have been studied by Najem (Al-Najem et al.1993, 1993a) and by Atkins (Atkins et al., 2008)

The effect of buoyancy forces to maintain stable the stratification between hot and cold molten salts in the same tank (Sanderson and Cunningam,1995), (Mawire and McPherson,2009), (Singh, et al 2010).

Another low cost effect, in a single tank is the used filler material which is not expensive and acts as the primary thermal storage medium (Price, 2003), (Kearney et al, 2001).

As Pacheco (Pacheco et al, 2002), Brosseau (Brosseau et al, 2005) presents a detailed list of the more adequate filler materials storage properties to retain the thermocline tanks energy.

(Yang and Garimella, 2010) developed a computed fluid dynamics model of a molten salt thermocline tank to analyze multi-dimensional effects.

Flueckiger (Flueckiger et. al., 2010, 2011), and Garimella (Yang and Garimella, 2010) updated the model to include several other effects like convection losses at the tank wall to the ambient, effect of the Reynolds number, effect of prolonged cooling of salt near walls, convection effects and radiation losses. A parametric study of filler-bed granule diameter and external convection losses assess the influence on the first and second law cycle efficiencies.

Rocio (Rocio and Rojas, 2013). develop work essential to allow the comparison and validation between numerical results of different authors.

The present work shows an analysis of the effect of different values for porosity filler together wither different aspect ratios for a thermocline considering a given profile of energy and temperature charge/discharge for a day. The analysis is based on a 2D model validated previously validated with literature data. Results are obtained through ANSYS®16 with the help of some extra C programming for Boundary Conditions. Residuals instabilities are well prevented by the employed methods of integration and Péclet number guaranties numerical instability as well.

2. Model Description of a 2D Storage System

A simple representation of the thermocline tank is presented in Figure 1. The tank is filled with a porous media and a liquid phase based on molten salt. The molten salt flow allows energy transfer inside the tank occupying all the voids existing between solid parts.

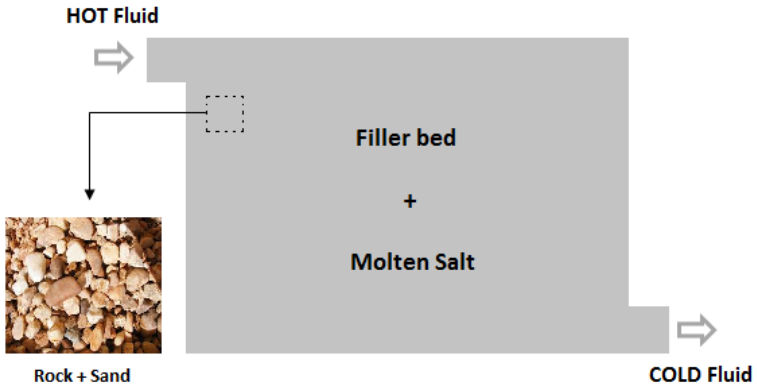

Fig. 1- Thermocline Scheme

The density, viscosity and thermal conductivity of the molten salt are defined by the following temperature T in Celsius dependent functions derived from experimental data (Rojas, 2013):

$$\rho(T) = -0.713\ T + 871.1 \qquad [\text{kg/m}^3] \qquad (1)$$

$$\nu(T) = 0.0452\ (T^{1.943}) \qquad [\text{m}^2/\text{s}] \qquad (2)$$

$$k(T) = -0.00014\ T + 0.125 \qquad [\text{W/m}^{2\text{o}}\text{C}] \qquad (3)$$

Thermocline tank characteristics are summarized in Table 2.

Table 2 – Tank characteristics

Properties	Tank
Height h [m]	15.3
Width l [m]	23.5
Tmax [°C]	550
Tmin [°C]	290
Porosity of the filler ε	0.22

Thermocline storage media properties are expressed in Table 3 where molten salt represents the eutectic mixture 60% $NaNO_3$ and 40% KNO_3 (trade name HITEC) and the filler is a mixture of rock and sand (Rojas, 2013).

Table 3 - Table Thermocline Storage Media properties

Properties	Molten salt	Filler
Thermal conductivity k (W/m ^oC)	0.54	2.4
Density ρ (kg/m^3)	1857	2690
Heat capacity by unit volume ρ Cp (kJ/m^3 ^oC)	2785	2260
Specific heat Cp (kJ/kg ^oC)	1.5	0.84

3. Governing Equations

The numerical model considers a porous storage field material where a flow enters the tank.

The porous media model in CFD ANSYS (ANSYS® 14) can be used for a wide variety of problems namely when a flow enters through a packed bed. The model incorporates an empirical determined flow resistance in a region defined as porous. They are recognized by some conditions:

- The porous media model assumes that the porosity is isotropic, and it can vary with space and time.
- The superficial velocity is based on the volumetric volume flow rate to ensure the continuity of the velocity vectors across the porous media interface.
- Porous media are modeled by the addition of a momentum source term to the storage fluid flow equations. The source term is composed of two parts: a viscous loss term (Darcy, the fourth term on the right-hand-side eq. 5) and an inertial loss term (the last term on the right-hand-side eq.5).
- The momentum contributes to the pressure gradient in the porous cell creating a pressure drop that is proportional to the fluid velocity (or velocity squared) in the cell.
- Molten storage is treated as a Newtonian incompressible fluid and the heat is conducting according to the Fourier law and being subjected to a gravitational field. The viscosity is assumed to vary with the temperature.

3.1 – Equations for mass and momentum transfer

Mass and momentum transport of the molten salt in the filler bed are governed according (Launder and Spalding, 1972) by:

$$\frac{\partial(\varepsilon\rho_l)}{\partial t} + \nabla.(\rho_l v) = 0 \quad (4)$$

$$\frac{\partial(\rho_l v)}{\partial t} + \nabla.\left(\rho_l \frac{vv}{\varepsilon}\right) = -\varepsilon\nabla.p + \nabla.\mathbf{T} + \varepsilon\rho_l\vec{g} - \varepsilon\left(\frac{\mu}{K}v + \frac{F}{\sqrt{K}}\rho_l|v|v\right) \quad (5)$$

where **T** is denoting the viscous stress tensor as

$$\mathbf{T} = 2\mu S \quad (6)$$

with

$$S = \frac{1}{2}\left(\nabla v + (\nabla v)^{\mathrm{T}}\right) \quad (7)$$

In equation (5) the last term of righthand side (RHS) accounts for the viscous and internal drag forc ,2011), where: K and *F* denotes respectively the permeability and the inertial coefficient (Murthy et al., 2004) and (Beckermann, 1988) by:

$$K = \frac{d_m^2\,\varepsilon^3}{175\,(1-\varepsilon)^2} \quad (8)$$

$$F = \frac{1.75}{\sqrt{150\varepsilon^3}} \quad (9)$$

The mass transport equation (4) is exact. The second equation (5) is obtained from the former considering the Boussinesq approximation (Beckermann, 1988).

Equations (4) and (5) are related with thermal diffusion and convection inside the tank and are solved with the Standard k-ϵ model (ANSYS® 16)

3.2 –Equations for Energy conservation

Equations for the energy transport of the molten salt (with the subscript l if liquid) and solid filler (with the subscript s) and are expressed in eq. (10) and (11) close the model. The equations are coupled by the interstitial heat transfer coefficient h_i, where i denote the l or s subscripts.

$$\frac{\partial\left(\varepsilon\rho_l\, C_{pl}\, \mathrm{T}_l\right)}{\partial t} + \nabla.\left(\rho_l v\, C_{pl}\mathrm{T}_l\right) = \nabla.(k_s\nabla\,\mathrm{T}) + p\nabla.v + h_i(\mathrm{T}_s - \mathrm{T}_l) + \mathrm{tr}\left[\nabla\left(\frac{v}{\varepsilon}\right).\mathrm{T}\right] + \frac{vv}{2\varepsilon}\times\frac{\partial(\rho_l)}{\partial t} \quad (10)$$

$$\frac{\partial}{\partial t}[(1-\varepsilon)\rho_s Cp_s(\mathrm{T}_s)] = -h_i(\mathrm{T}_s - \mathrm{T}_l) \quad (11)$$

3.3 Initial and Boundary conditions

3.3.1. Initial conditions

The initial condition, corresponds to the tank at the cold stage, completely discharged with a temperature of 290ºC. The charge of the tank is done with the flow of molten salt at 550ºC at the inlet. Initial velocity inside the tank is zero. Outside the tank, the ambient temperature of the atmosphere is fixed at 27ºC.

The wall tank material is built in steel, with a constant roughness wall of 0.5m and thus induces shear stress along the walls.

3.3.2 Boundary conditions

Boundary conditions comprise the inlet, the outlet and the wall of the tank. At both inlet and outlet mass momentum and thermal conditions must be analyzed.

At the Inlet and Outlet

Thermal conditions are of Darcy type (imposed value). During charge T=550ºC and during discharge T= 290ºC, for inlet and of first order for outlet.

Momentum: according to the Charge/Discharge profile according a profile written in C and coupled to the program.

At the walls

Thermal: heat flux.

Momentum: There is a stationary momentum and a no- slip condition.

3.4 Model and Stability

3.4.1 Turbulence model Model

k-ϵ model, used in ANSYS is a two equation model which gives a general description of turbulence by means of two transport equations (PDEs), in this case equations (4) and (5).

The exact k-ϵeqations have a lot of terms some of them not measurable. For a practical approach some models were proposed by Launder (launder and Spalding, 1974), who minimizes the unknowns presenting a set of equations that can be applied to a large number of situations. For turbulent kinetic energy k:

$$\frac{\partial(\rho k)}{\partial t} + \frac{\partial(\rho k \mu_i)}{\partial x_i} = \frac{\partial}{\partial x_j}\left[\frac{\mu_t}{\sigma_k}\frac{\partial k}{\partial x_j}\right] + 2\mu_t E_{ij} E_{ij} - \rho\epsilon \quad (12)$$

For dissipation ϵ:

$$\frac{\partial(\rho\epsilon)}{\partial t} + \frac{\partial(\rho\epsilon u_i)}{\partial x_i} = \frac{\partial}{\partial x_j}\left[\frac{\mu_t}{\sigma_\epsilon}\frac{\partial\epsilon}{\partial x_j}\right] + C_{1\epsilon}\frac{\epsilon}{k}2\mu_t E_{ij}E_{ij} - C_{2\epsilon}\rho\frac{\epsilon^2}{k} \quad (13)$$

With u_i the velocity component in the corresponding direction; E_{ij} the component of rate deformation. The turbulent or eddy viscosity (μ_t) can be obtained combining ϵ, and k, and the values of the constants C as follow:

$$\mu_t = \rho C\mu\frac{k^2}{\epsilon}$$

The default values $C_{1\epsilon}$=1.44, $C_{2\epsilon}$=1.92,$C\mu$ =0.09 have been determined by numerous iterations of data fitting for a wide range of turbulent flows. The values for the constants here considered are not particular to the model here descripted but considered acceptable for the problem in question (ANSYS® 16).

3.4.2 Stability Criteria

The employed mesh to solve the problem is structured, and had in account the Péclet number (Fabrice, 2014) to avoid numerical instabilities. Numerical simulation methods, like Finite Element Method (FEM) requires stabilization procedures when modeling transport applications.

In these problems numerical instabilities can occur when approaching the solution, leading eventually to oscillations. Péclet number relates the convective and diffusive effects together with the mesh element size (Medina *et al*, 2007) through the no dimensional number Pe = $\frac{||v||d_m}{2\,\alpha}$, with v a generic convective velocity vector, α a generic thermal diffusivity effect and d_m the mesh element size.

Pe >1 numerical instabilities can occur as convective effects dominate diffusive activity; Pe<<1 is diffusion that dominates the process (which is not the case in a thermocline with filler)

Traditionally, the stabilization methods allow the construction of coarser meshes capable to simulate with enough accuracy all physic properties derived from the convective and diffusive phenomena. This leads to a more robust and faster computational performance.

3.5. Procedure

The governing transport equations were solved through finite volume element method using software (ANSYS® 16). The Initialization method chosen was the standard

initialization and the solution is computed from inlet zone. The solution method was a PISO algorithm coupled with a Pressure Velocity scheme. Pressure, momentum turbulent kinetic energy and time were discretized by a second order upwind scheme. Turbulence dissipation rate was discretized by a first order upwind scheme iterations at each time step ended when the dimensionless residual for all equations dropped below 10^{-5} (accuracy convergence). The solution problem was done with double precision. The domain of simulation here studied, was discretized into 10 418 cells (the mesh). The simulation run in a parallel system machine with 32GBytes of RAM with 4 Intel-Xeon dedicated processors. The programmed time-schedule for charge and discharge cycles in the tank was defined according to procedures presented in section.

3.6 Model Validation

In order to validate the thermal model, data from Solar One reported by Rojas (Rojas, 2013) was considered. The experimental data collected corresponds to a discharge process starting from a state in which the thermocline is located at the middle of the tank height. Observed temperature profiles were done during a discharge process at 0:00 AM, 4:00 AM and 8:00 AM, are shown in Figure 2. The 2D Thermocline modelling procedure presented in section 3 was used to simulate the results from Solar One. These results are presented in Figure 2 together with the data from Solar One tank mentioned above. The obtained results by the model are in good agreement with the observed data.

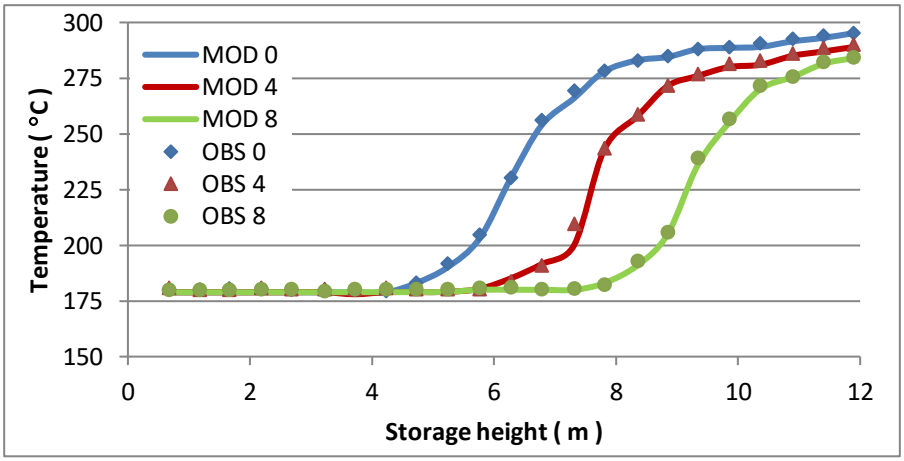

Fig. 2- Solar One data (OBS – observed) vs 2D numerical results (MOD - modelling)

4. Considered Profile.

The following profile is presented in Figure 3 and was designed according to a real CSP plant charge/discharge process. It has a first and unique charge process for eight and a half hours of 45 kg/s followed by a discharge of six hours with a mass flow of 67 kg/s. At the end a deeper discharge process of 190 kg/s was considered. Figure. 3 illustrate the charge flow rate in the inlet and the discharge rate at the outlet.

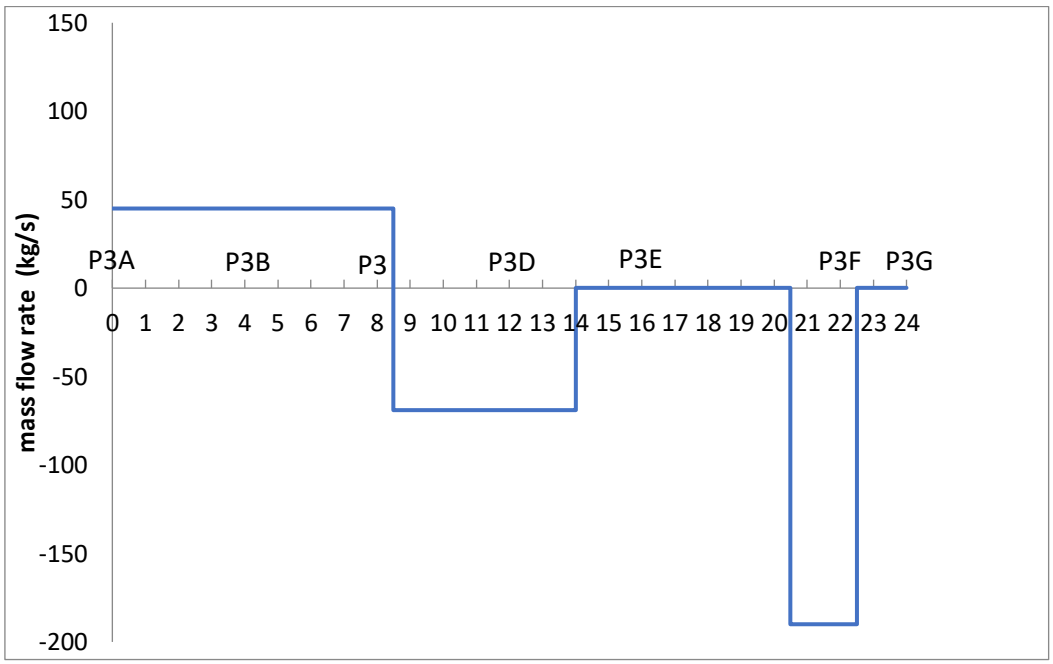

Fig. 3 -Profile of rate mass flow for a day

Temperature profiles for the points P3A=0h; P3B=4h: P3C=8h; P3D=12h; P3E=16h, P3F=22h and P3G=24h can be seen in Figure 4.

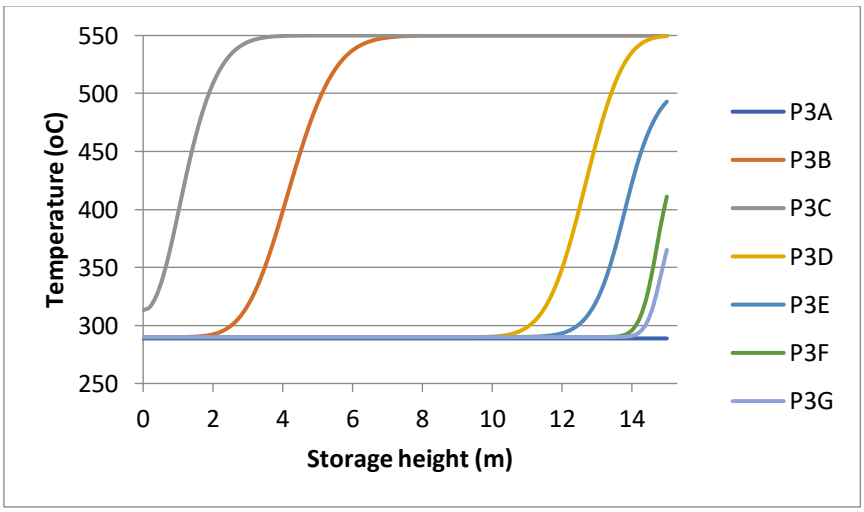

Fig. 4-Temperature Profiles

The process starts with the tank at 290 ºC. The charge is done very slowly and takes eight hours. The discharge is quickly and gives rise to two convective cells. The discharge continues and the tank enters in a platform of rest corresponding to a situation where there is no energy extraction. This period of time takes six hours during which there is a compromise between the hot and cold layers. The process of degradation of the hot layer becomes greater until fourteen hours where discharge ends. At this time the tank becomes resting and two big convection cells are formed.

A new discharge begins for two hours and finally a new situation of rest, Figure 5d), where the process in the tank ends completely discharged.

This profile is similar to the behavior demand of a real CSP plant as it begins with a great charge and during the rest of the day only two other situations can occur: discharges or nothing. The tank begins cold and ends cold, that is an all entire charge/discharge cycle is completed.

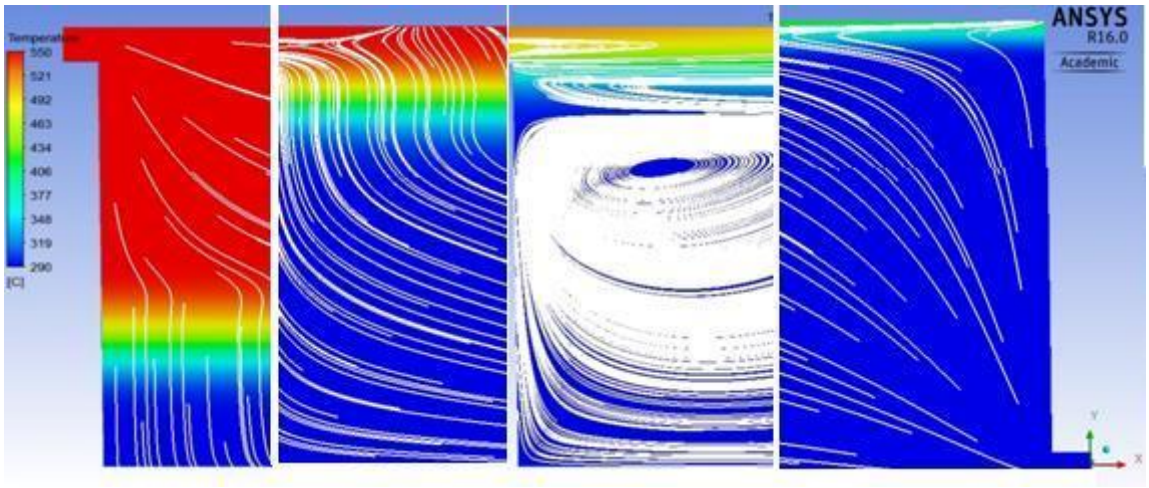

Fig. 5- Temperatures and Streamlines for the situations:

a) PB=4h, b) PD= 12h, c) PE=16h, d) PF=22h:

The behavior of the TES is perfect and thermocline shows temperature evolution when dealing with a porous media. A complete cycle is reached. The tank begins cold, then is completely charged and ends cold again after the discharge process.

It may be noted that in situations of no enter /exit of fluid in the tank, convection cells tend to form due to the continuity of the fluid movement, that is, to the need of the fluid to move and revert the process. The velocity values are very low (order of $2x10^{-2}$ m/s) in **this case but the phenomena can contribute to the destabilization of the layers and** consequently contribute to the degradation of the tank stratification.

The storage device suffers two peak of extraction that corresponds to the beginning and the end of the day where the extraction of energy demand is higher. The charge occurs during the solar hours and for the rest of the day the tank works like a storage device. In this context, the tank works effectively as a storage device.

5 Porosity analysis

5.1. Introduction

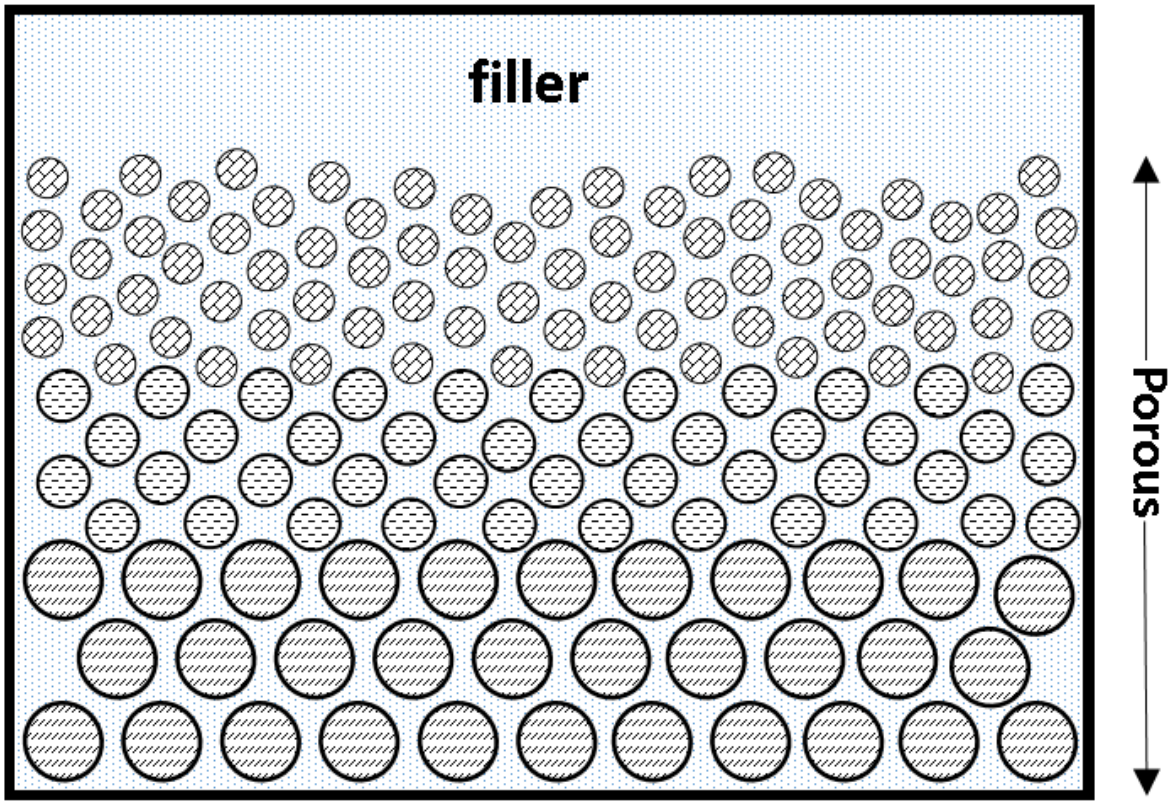

Fig. 6- Considered porosities

The knowledge of the size of filler bed particles is very important for a thermocline design. Porous media pores are adjustable to a certain degree of voids that allowed the hot molten salt to reach the tank and thus to contribute to a full developed thermocline.

Permeability is an important concept for a given porous media concerning momentum transport as it is one of the factors that must be known for numerical simulation. This property is often treated in an easily way as porosity or void fraction. The thermal dispersion caused by a solid media plays an important role in the heat transfer enhancement.

Considering the heat storage tank with the filler material and the heat transfer fluid, the void fraction is the ratio of the volume occupied by the fluid as follows;

$$\varepsilon = \frac{V_f}{V_{tank}} \qquad (14)$$

Where, as referred, ε means porosity.

This effect is related with materials properties of the filler and with the pretended demand thermal energy storage of the plant.

5.2 Comparison of three values for porosity of filler

Three values for the porosity were taken into account; ε = 0.14, ε = 0.22 and ε = 0.46. The first one is considered the lower limit and the last one is taken as a higher possible value for porosity. Their performance was analyzed at 4h, 12h, 16h and 22h.

The purpose is to analyze which is the value that contribute to a better develop of the thermocline and consequently to reach a higher temperature.

Fig. 7 Porosities for situation of H/W<1

Figure 5 allows to take some conclusions about the situation where in the tank the considered geometry is H/W <1 (Height/Weight).

An evidence of Figure 7 is that higher temperatures are obtained when the porosity of the filler bed is higher (ε =0.46). At this situation the thermocline is less defined. Discharge

efficiency is increased by smaller filler-bed particles that are in the tank where are more voids. The filler can move very quickly and in a very free way through the rocks. It is impossible to establish a thermocline, and a great discharge is not always desirable

The situation that corresponds to better defined thermoclines is when ε =0.14. The situation is the inverse of the first one but, however, it could not be the ideal. The intermediate situation, ε =0.22, can be a good compromise between a well- defined thermocline and a reduced loss of charge, in order to obtain a better storage unit functioning.

Fig. 8-Amplification for the results of 16h and 22h for T in [300, 400][oC]

Figure 8 clearly shows the difference of temperatures when considering the porosities of 0.14, 0.22 and 0.46 for 16h and 22h in the range of 300 to 400 degrees. Temperature profiles for lower values of porosities are almost parallel being the profile for 0.14 more straight. This profile as well as the one corresponding to 0.22 conducts to higher temperatures than the one corresponding to 0.46.

5.3 Aspect Ratio effect

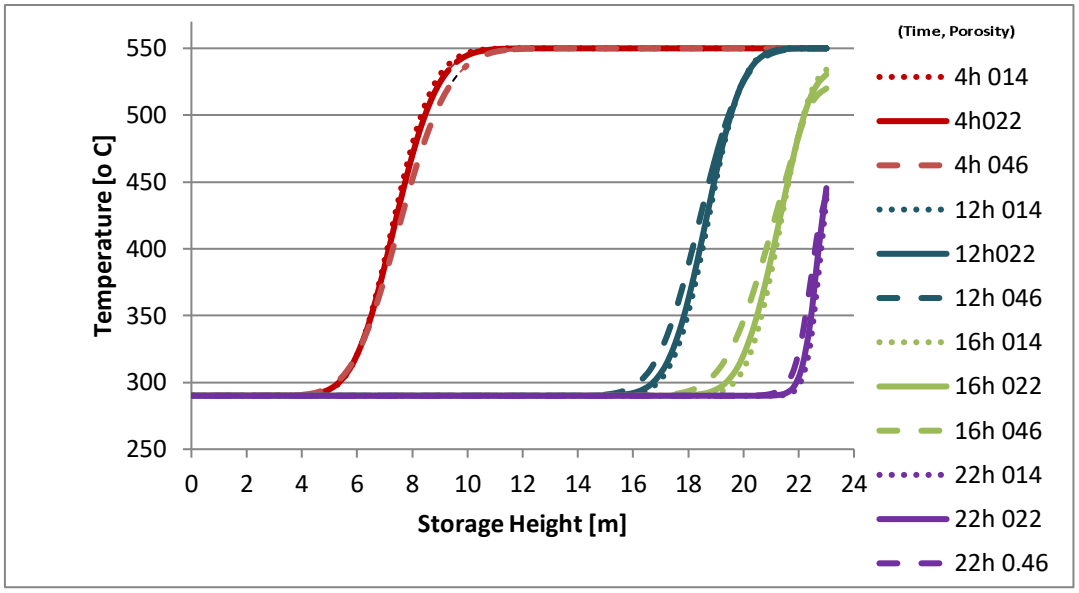

Fig. 9. Porosities for situation of H/W >1

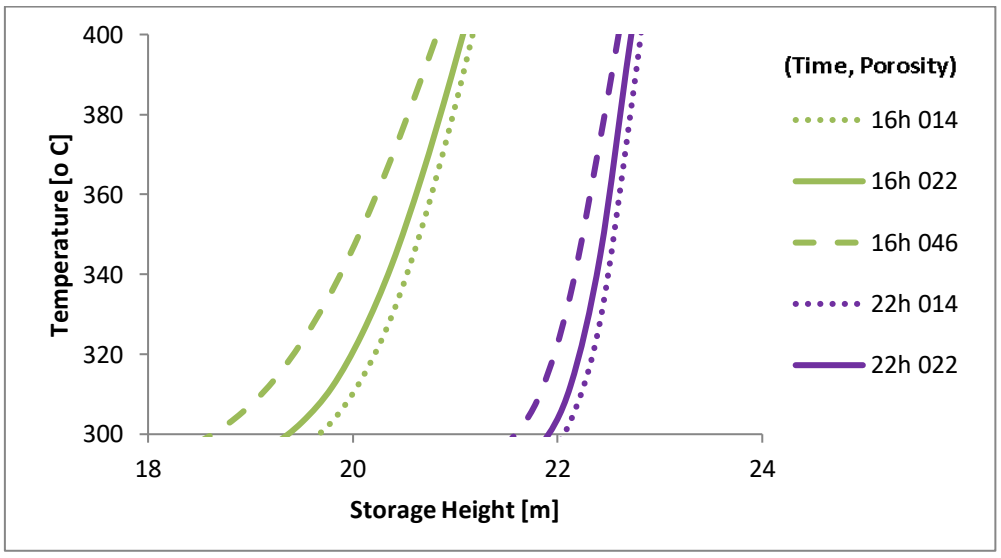

Fig. 10 Temperature Profiles considering16h and 22h for T in [300, 400][oC]

When the tank is higher than large the achieved temperatures for all the tested porosities are almost identical between them. In this case the heat exchange layer expands greatly. Since the molten salt temperatures in the gradient zone are lower than the constant high temperature level, expanded layer reduces the amount of high temperature molten salt delivered and thus decreases the discharge.

In this situation, H/W >1, it can be seen that the effect of a vertical geometry is more important in stratification than the effect promoted by different porosities.

The temperatures that are obtained are higher than with the other configuration (see Figure10)

6. Conclusion

Three porosities were tested in order to infer about the existence of voids in the molten storage thermocline. The better developed thermoclines are those obtained with less voids but in this case the discharge are not so efficient. The situation of a more efficient discharge is when the porosity is higher which sometimes is not desirable for a plant demand. The conclusion is that an intermediate situation will provide well developed thermoclines and will correspond to a pretended charged as a function of a plant demand.

If the aspect ratio is also considered, the effects of the porosities disappear faced to the geometry. Large thermoclines do not registry the effect of different porosities. Higher tanks are ideal for storage and well defined thermoclines. So the geometry is more important to consider than porosity when designing a molten storage thermocline.

A thermocline storage system should be designed with a large height and operate at a low discharge power in order to have a higher discharge efficiency, with a porosity that obeys to those conditions, thus corresponding to the plant demand.

REFERENCES

Angelini G. Lucchini A. Manzolini G. 2014. Comparison of thermocline molten salt storage performances to commercial two tank configuration. Energy Procedia. 49, pp..694-704.

ANSYS® Academic Research, Release 14.0, In: Chapter 12.1.4; Release 16.0, In: Chapter 6.2.3.7.

Al-Najem N. 1993. Degradation of a stratified thermocline in a solar storage tank. Int. J. Energy Res., Vol .17, pp. 183-191.

Al-Najem, N, Al-Marafie, A.M. and Ezuddin, K.Y, 1993. Analytical and experimental investigations of thermal stratification in storage tanks. Int. J. Energy Res. Vol. 97, pp. 77.

Atkins M.J., Morrison, A.S. and Walmsley, M.R., 2008. Stratified Tanks for Heat Storage – Interface Control and Re-establishment. CHEMECA Conference, New Castle, Australia, September.

Bayon, R. and Rojas, E.2013. Simulation of thermocline storage for solar thermal power plants: From dimensionless results to prototypes and real-size tank. Int. J. Heat Mass Trans. Vol. 60.

Beckermann, C. and Viskanta, R.1988. Natural convection solid/liquid phase change in porous media. Int. J. Heat Mass Trans.Vol.31. pp.35-46.

Brosseau D. et al.2005. Testing Thermocline Filler Materials and Molten Salt Heat Transfer Fluids for Thermal Energy Storage Systems in Parabolic Trough Solar Power Plants. Journal of Solar Energy Engineering, 127(1), pp.109-116.

Fabrice S. 2014. Understanding Stabilization Methods, COMSOL, May.

Flueckiger S., Yang Z., Garimella S.V. 2010. Thermocline Energy Storage in the Solar One Power Plant: An Experimentally Validated Thermo-mechanical Investigation. Proceedings of the ASME Int. Conf. Energy Sustainability. Beijing. China.

Flueckiger S, Yang Z. and Garimella S.V. 2011. Integrated Thermal and Mechanical Investigation of Molten- Salt Thermocline Energy Storage. CTRC Research applications, Appl. Energy. Vol.88.

Gross R. I. 1982. An experimental study of single medium thermocline thermal-energy storage. ASME Paper 82 HT-53.

Mawire A.,McPherson M.,van der Heatkamp RRJ.,Mlatho SJP..2010Simulated performance of storage materials for pebble bed thermal energy storage (TES) systems. Appl. Energy. 2009. 86.pp.1246-52

Price H., 2003. A parabolic trough solar power plant simulation model.

Sanderson, T.M., Cunningham, G. T., 1995. Performance and efficient design of packed bed thermal storage systems. Part I. Appl. Energy. 50,119-132

Singh H., Saini, R. P., Saini, J. S. 2010. A review on packed bed solar energy solar systems. Renew. Sustain. Energy. Rev. 14(13). Pp. 1059-1069.

Kearney and Associates, 2001. Engineering evaluation of molten salt HTF in a parabolic through solar field. NREL Contract No NAA-1-30441-04.

Kolb G.J. 2006. Performance analysis of Thermocline energy storage. Proceedings of ISEC, ASME Int. Solar Energy Conference, July 8-13, Denver, USA.

Krishnan S, Murthy J.Y. and Garimella S.V. 2004. A two temperature model for analysis of passive thermal control system. ASME Journal Heat Transfer Vol. 126. pp. 628-637.

Launder B.E and Spalding D.B. 1972. Lectures in mathematical models of turbulence. Fourth Academic Press, London, England.

Pacheco J. E. Showalter S.K. and Kolb J. 2002. Development of a Molten-Salt Thermocline Thermal Storage System for Parabolic Trough Plants. Journal. of Solar Energy Engineering, 124(2), pp. 153.

Yang Y. and Garimella S.V. 2010. Molten-Salt Thermal Energy Storage in Thermoclines under Different Environmental Boundary Conditions. Appl. Energy. Vol. 87.cc